EGTRIB Journal
JOURNAL OF
THE EGYPTIAN SOCIETY OF TRIBOLOGY
VOLUME 22, No. 1, January 2025, pp. 23 - 33 **ISSN 2090 - 5882**
(Received August 28. 2024, Accepted in final form October 25. 2024) **jest.journals.ekb.eg**

PROPER MATERIALS FOR THE FRICTION SURFACES OF THE TRIBOELECTRIC NANOGENERATOR

Ali A. S.[1], Zeinab A. H.[2], Al-Kabbany A. M.[2, 3] Ali W. Y.[2] and Abdu H. M.[2]

[1]Mechanical Engineering Dept., Faculty of Engineering, Suez Canal University, EGYPT,
[2]Department of Production Engineering and Mechanical Design, Faculty of Engineering, Minia University, Minia 61111, EGYPT,
[3]Smart Biomaterials and Bioelectronics Lab, National Taiwan University, TAIWAN.

ABSTRACT

The present work aims to develop the efficiency of bidirectional direct current triboelectric nanogenerator (BDC-TENG). Different materials such as aluminium (Al), polyamide (PA) and Kapton films adhered to polymethyl methacrylate (PMMA) cube as moving friction surfaces were tested. They were sliding on the stationary PMMA, poly propylene (PP) and silicon rubber (SR) in order to harvest the generated voltage to be applied as feedback signal of the self-powered sensor used in the electronic skin (e-skin).

It was found that among the tested materials used as moving and stationary friction surfaces, Al sliding on SR recorded the highest voltage. Besides, Kapton slid on PMMA showed significant voltage increase with increasing the intensity of the magnetic field when permanent magnets were inserted under the stationary surface. Further voltage increase was observed when the magnets were wrapped by copper coil. In contradiction to that, sliding of Al on PP generated relatively lower values. Further voltage increase observed when the magnets were wrapped by copper coil. It can be concluded that the proposed BDC-TENG can be applied as a self-powered sensor in the application of the e-skin design due to the function of the proposed BDC-TENG that generated bidirectional voltage, where the flow of the direct current in the external circuit in two directions during sliding.

KEYWORDS

Triboelectric nanogenerator, polymers, feedback signal, sensor, electronic skin, permanent magnet.

INTRODUCTION

The development of the double-channel bidirectional direct current triboelectric nanogenerator (BDC-TENG) is essential to enhance the performance of the system of the electronic skin (e-skin). BDC-TENG was proposed using polymers like polymethyl methacrylate (PMMA) and polyamide (PA) textiles and strings as well as metallic ones like aluminium (Al) and copper (Cu) films as friction surfaces sliding

on polytetrafluoroethylene (PTFE) film to generate the feedback signal to operate the e-skin. Besides, the thickness of the friction surfaces was investigated, [1, 2].

The effect of the induction of the magnetic field on ESC generated by the proposed TENG was investigated, [3 - 10]. It was found that the moving electrode that cut perpendicularly the highest number of the magnetic field lines produced the highest ESC. In addition to that, the direction of sliding showed significant effect on ESC. The performance of the TENG based on triboelectrification and induction made by magnetic field depends on the strength and the place of the permanent magnets relative to the contact area. The insertion of the steel sheets between the permanent magnets and the contact area can distribute the lines of magnetic field, because the steel sheets can redirect the magnetic field lines of the magnet and provided extra magnetic field, where that effect depends on the sheet thickness.

The drawbacks of triboelectrification are destruction of electronics and fires, [11 - 15]. In order to reduce that effect, it was found that, the sliding materials should be blended by others of different charges, [16 - 18]. In hospital and medical field, triboelectrification can be applied to repel viruses, [19 - 23], and develop the performance of TENG, [24 - 26]. Triboelectrification supported by electrostatic induction could enhance the efficiency of TENG in energy harvesters, [27 - 30], sensors, [31 - 33], as well as electromagnetic TENG, [35 - 38].

In the present work, different materials such as Al, PA and Kapton films as moving friction surfaces sliding on the stationary ones of PMMA, PP and SR in order to get the highest voltage output were tested.

EXPERIMENTAL

The proposed BDC-TENG consisted of the moving surfaces that consisted of PMMA cube of 20 × 20 × 20 mm^3 coated Al, PA and Kapton films of 25 μm thickness. The stationary surfaces were PMMA, PP and SR. Two charge-collecting electrodes made of copper sheet were adhered to the two sides of the moving PMMA cube, Fig. 1. Permanent magnets of 120 and 240 mG field intensity were inserted under the stationary sheets, Fig. 2. The permanent magnets were wrapped by copper coil of 0.2 mm diameter and 25 turns to strengthen their induction, Fig. 3. An Arduino-Uno was used to measure the generated ESC in mV during sliding on the two sliding surfaces in two directions. The average of the voltage peaks during the test run measured by the electrodes was determined.

The load values were 0.3, 2.3, 4.3, 6.3, 8.3 and 10.5 N. The sliding distance was 10 mm. The function of the BDC-TENG is to generate double signal voltage depending on the sliding direction. The movement of the friction surface to the right makes electrode I to collect ESC from the stationary friction one, Fig. 1, and electrode II collects ESC in different signal when the movement turns to the left direction.

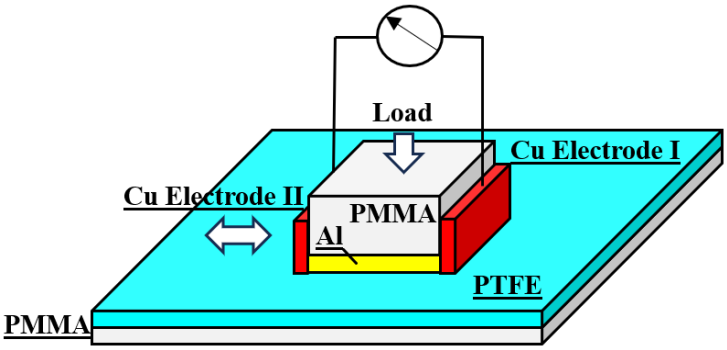

Fig. 1 Arrangement of the test procedure.

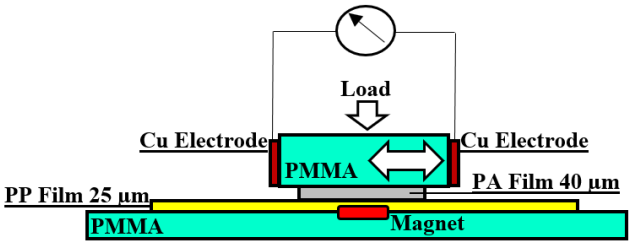

Fig. 2 Arrangement of the tested TENG provided by permanent magnet.

Single magnet wrapped with copper coil (120 mG). **Two magnets wrapped with copper coil (240 mG).**

Fig. 3 Arrangement of the magnets wrapped by copper coil.

RESULTS AND DISCUSSION

The sliding of Al film on PMMA, SR and PP induced voltage difference between the two electrodes. Figures 4 and 5 illustrate the voltage values generated in the two directions versus time when Al slid on SR and PMMA respectively at 3.3 N load. The function of the proposed BDC-TENG is to generate positive and negative voltages depending on the sliding direction. When Al surface moves to the right, electrode I collects ESC from SR or PMMA, Fig. 1. The left movement causes electrode II to collect ESC in different signal.

The comparative performance of the tested materials used as stationary friction surface is shown in Fig. 6. Generally, voltage significantly increased with the increase of the applied load. SR represented the highest voltage followed by PP and PMMA. That behavior can be explained on the bases of the triboelectric series that determines the polarity of the ESC of the sliding surfaces due to the electron transfer from one surface to the other, [40]. The materials listed in the upper part in the triboelectric series when slides on materials located in the lower part will be positively charged

while the lower one will be negatively charged. The magnitude of ESC depends on the distance between the two materials. Materials generate ESC during friction with each other, where the magnitude and polarity depend on their position in the triboelectric series. The higher positioned ones gain positive ESC, while the lower ones gain negative ESC. Figure 7 illustrates the triboelectric series where the materials are ranked. Because the distance between Al and SR is longer than that between Al and PP as well as Al and PMMA, therefore, the sliding pair Al/SR displayed the highest voltage as measure of the generated ESC. Based on that observation, it can be recommended that Al can be used in the moving friction surface and SR can be applied for the stationary one to harvest the highest voltage.

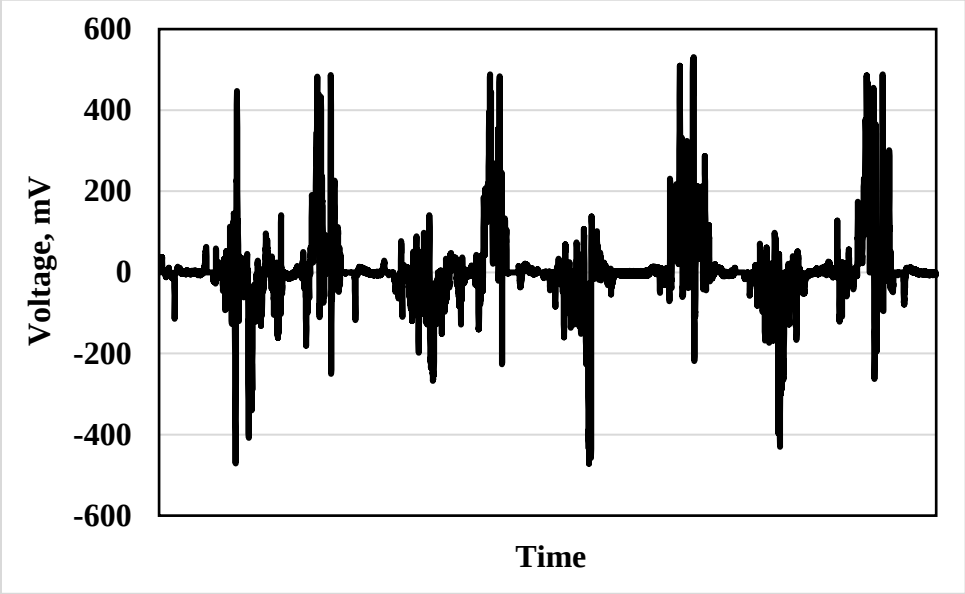

Fig. 4 Voltage generated from sliding of Al on SR versus time.

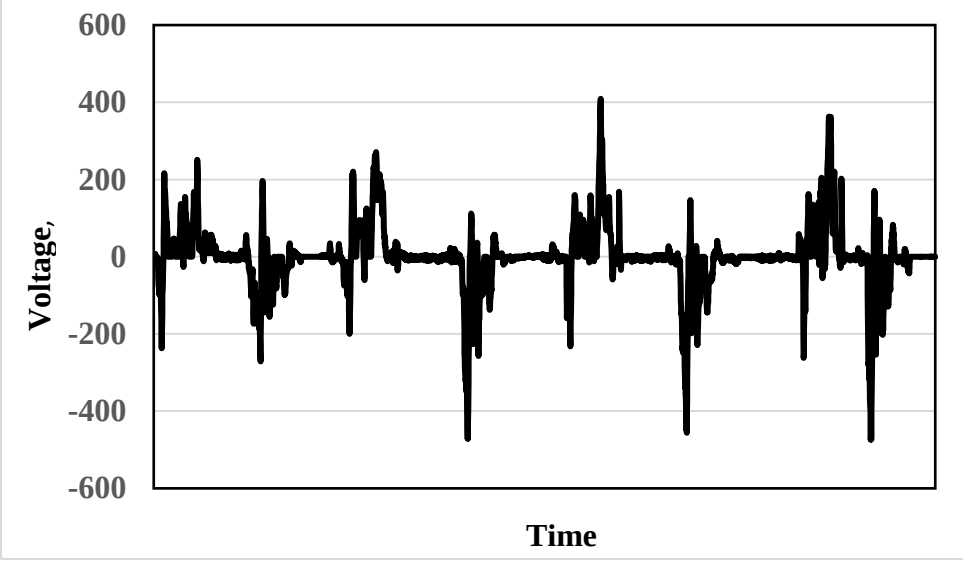

Fig. 5 Voltage generated from sliding of Al on PMMA versus time.

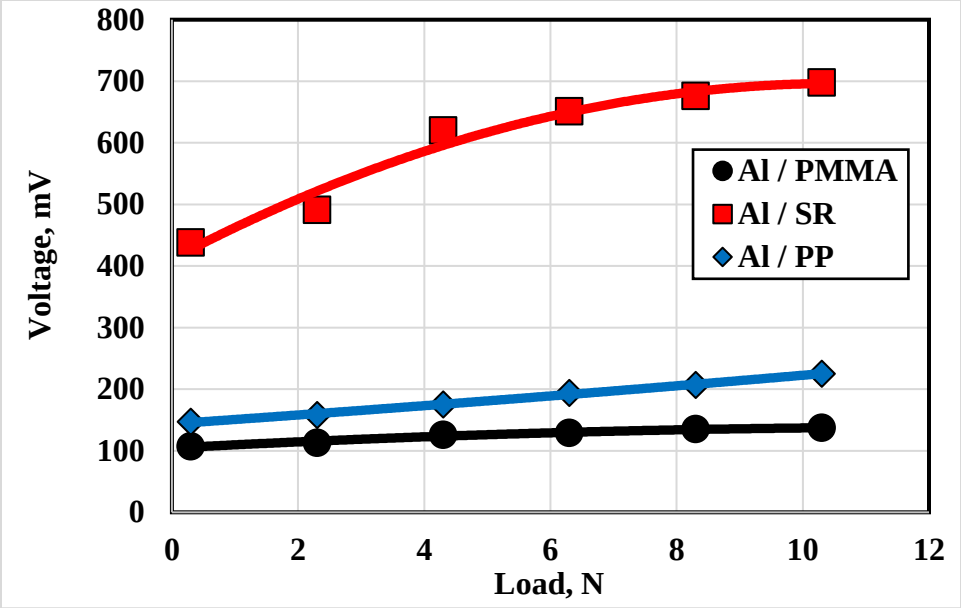

Fig. 6 Voltage generated from sliding of Al on PMMA, SR and PP.

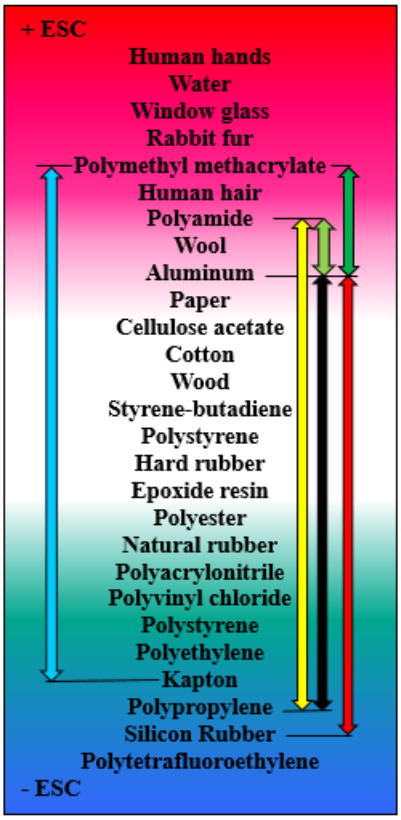

Fig. 7 Triboelectric series of the materials.

The moving friction surface was coated by Kapton slid on PMMA then the voltage was measured under the influence of the permanent magnet to enhance the efficiency

of the TENG. The results of the experiments are shown in Fig. 8. It was observed that voltage increased with increasing the magnetic field. The highest voltage values recorded 653 mV at 240 mG. Further voltage increase was measured when the magnets were wrapped by copper coil, Fig. 9, where the highest voltage recorded 686 mG. It seems that the induction of the copper coil increased the electric field and consequently voltage increased.

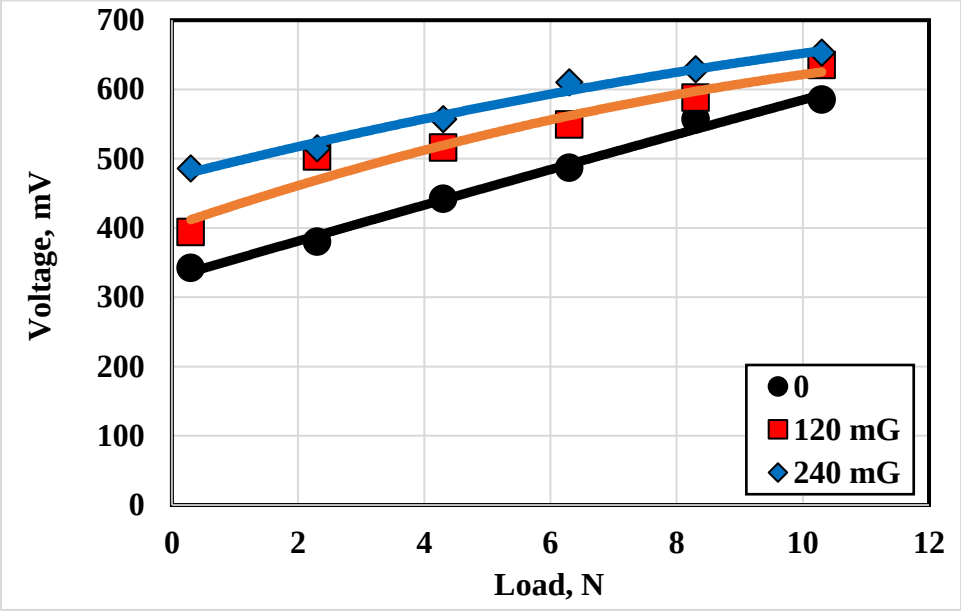

Fig. 8 Voltage generated from sliding of Kapton on PMMA under the influence of the permanent magnet.

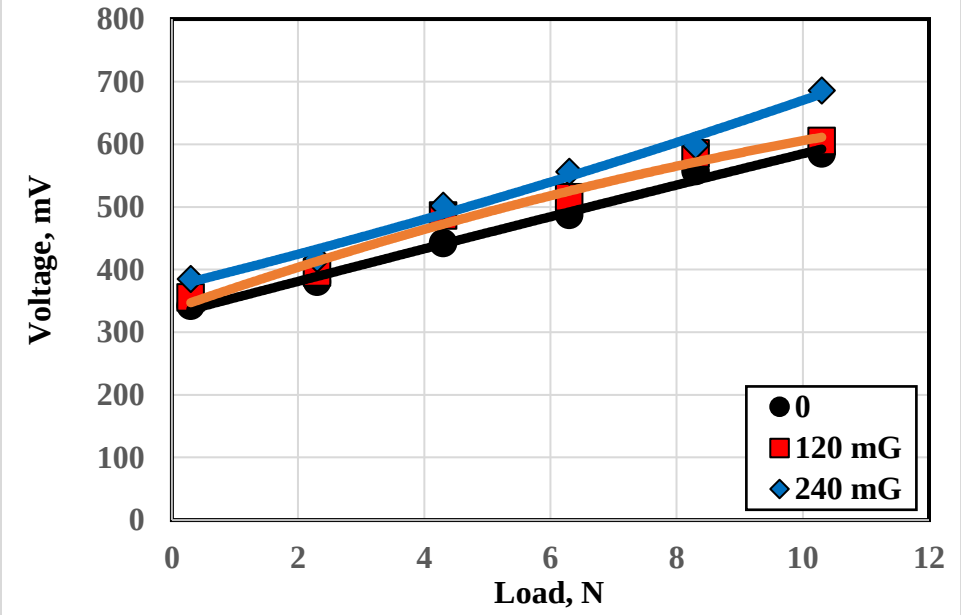

Fig. 9 Voltage generated from sliding of Kapton on PMMA under the influence of the permanent magnet wrapped with copper coil.

In condition of replacing Kapton by Al and PMMA by PP, the values of voltage generated from sliding of Al on PP under the influence of the permanent magnet is shown in Fig. 10. The values of voltage did not exceed 230 mV at 10.3 N although the distance between Al and PP in the triboelectric series is quite long. The insertion of magnets under PP substrate strengthened the intensity of the ESC induced magnetic field that increased the magnitude of the ESC, where the highest voltage value reached 297 mV at 240 mg magnetic field intensity. When the magnets were wrapped by copper coil, voltage increased, Fig. 11, where the highest voltage values increased up to 318 mV due to the increase of the induction of the magnetic field.

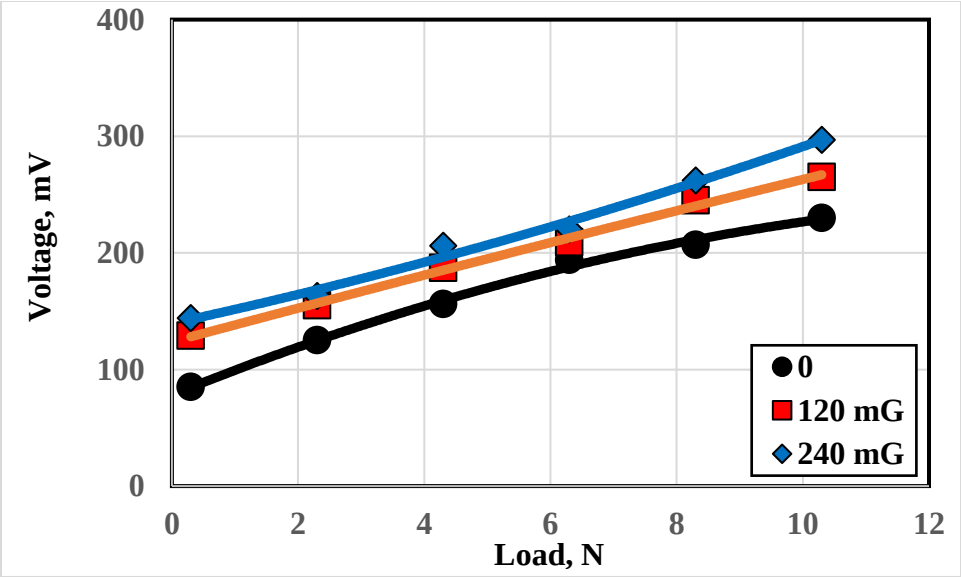

Fig. 10 Voltage generated from sliding of Al on PP under the influence of the permanent magnet.

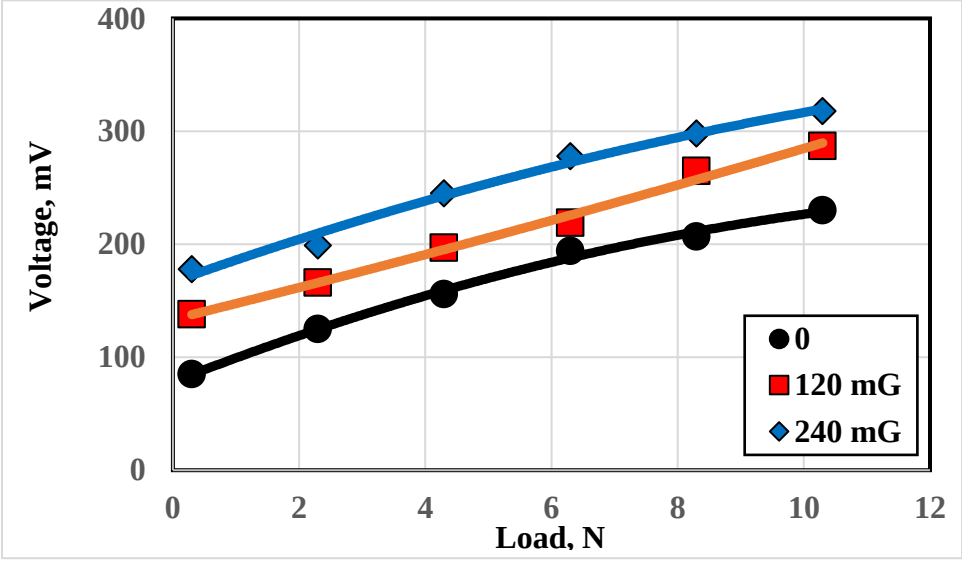

Fig. 11 Voltage generated from sliding of Al on PP under the influence of the permanent magnet wrapped by copper coil.

Voltage generated from sliding of PA on PP showed reasonable values increasing with the increase of the intensity of the magnetic field, Fig. 12. The highest values of voltage measured at 10.3 N load were 307, 464 and 532 mV at 0, 120 and 240 mG magnetic field intensity respectively.

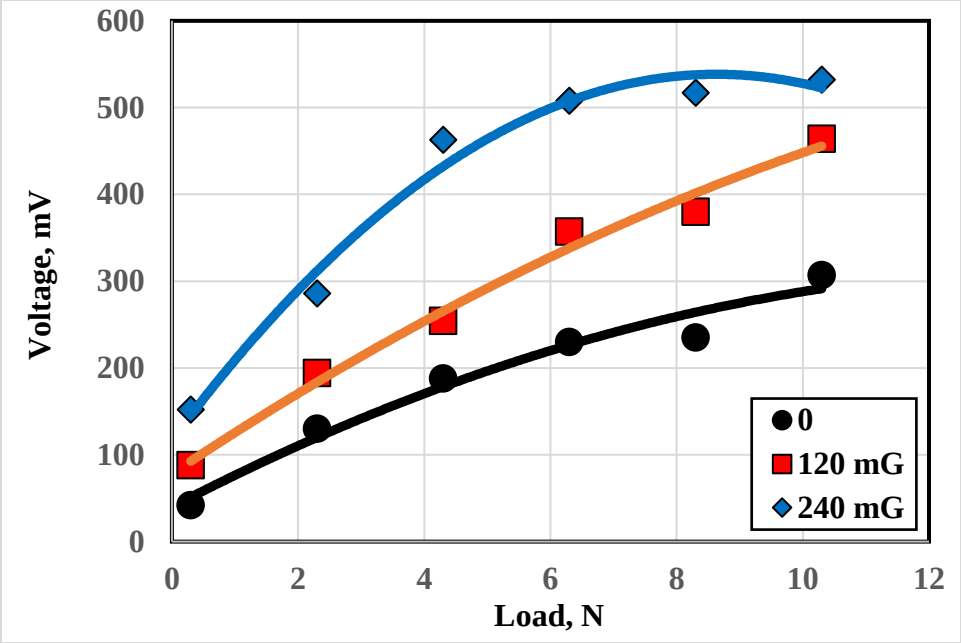

Fig. 12 Voltage generated from sliding of PA on PP.

Based on the observations in the present work, it is noticed that the proposed BDC-TENG generated bidirectional voltage, due to the flow of the direct current in the external circuit in two directions during sliding. That performance qualified the proposed BDC-TENG to be applied as a self-powered sensor in e-skin design.

CONCLUSIONS

1. SR represented the highest voltage followed by PP and PMMA when Al slid on them.
2. It can be recommended that Al can be used in the moving friction surface and SR can be applied for the stationary one to harvest the highest voltage.
3. Kapton slid on PMMA showed significant voltage increase with increasing the intensity of the magnetic field.
4. Wrapping the magnets by copper coil induced further voltage increase.
5. Sliding of Al on PP generated relatively lower values.
6. Inserting permanent magnets under PP substrate increased the voltage. Further voltage increase was observed when the magnets were wrapped by copper coil.
7. Based on the observations in the present work, it is noticed that the proposed BDC-TENG generated bidirectional voltage, due to the flow of the direct current in the external circuit in two directions during sliding. That performance qualified the proposed BDC-TENG to be applied as a self-powered sensor in e-skin design.

REFERENCES

1. Ali A. S., Al-Kabbany A. M., Ali W. Y. and Ameer A. K., "Bidirectional Direct Current Triboelectric Nanogenerator for Electronic Skin", Journal of the Egyptian Society of Tribology, Vol. 22, No. 1, January 2025, pp. 11 – 22, (2025).

2. Ali A. S., Al-Kabbany A. M., Ali W. Y. and Ameer A. K., "Development of Bidirectional Direct Current Triboelectric Nanogenerator", Journal of the Egyptian Society of Tribology, Vol. 21, No. 4, October 2024, pp. 71 – 81, (2024).

3. El-Shazly M. H., Al-Kabbany A. M., Ali W. Y., Ali A. S. and Ameer A. K., "Influence of Magnetic Field on the Performance of the Triboelectric Nanogenerator", Journal of the Egyptian Society of Tribology, Vol. 21, No. 1, January 2024, pp. 12 – 23, (2024).

4. El-Shazly M. H., Al-Kabbany A. M. and Ali W. Y., Ali A. S. and Massoud M. A., "Effect of the Direction of the Magnetic Field Lines on the Voltage Output of a Triboelectric Nanogenerator", Journal of the Egyptian Society of Tribology, Vol. 20, No. 4, October 2023, pp. 65 – 76, (2023).

5. El-Shazly M. H., Al-Kabbany A. M. and Ali W. Y., Ali A. S. and Massoud M. A., "Effect of the Direction of the Magnetic Field Lines on the Voltage Output of a Triboelectric Nanogenerator", Journal of the Egyptian Society of Tribology, Vol. 20, No. 4, October 2023, pp. 65 – 76, (2023).

6. Elzayady N., Al-Kabbany A. M., Ali W. Y., Ali A. S. and Hamdy K., "Enhancing the Performance of the Triboelectric Nanogenerator", Journal of the Egyptian Society of Tribology, Vol. 20, No. 4, October 2023, pp. 77 – 87, (2023).

7. Ali A. S., Youssef M. M., Ali W. Y. and Elzayady N., "Triboelectric Nanogenerator Based on Contact and Separation as well as Sliding of Polyamide on Polytetrafluoroethelene", Journal of the Egyptian Society of Tribology, Vol. 20, No. 1, January 2023, pp. 32 – 40, (2023).

8. Ali A. S., Youssef M. M., Ali W. Y. and Rashed A., "Enhancing the Efficiency of Triboelectric Nanogenerator by Electrostatic Induction", Journal of the Egyptian Society of Tribology, Vol. 20, No. 1, January 2023, pp. 41 – 50, (2023).

9. El-Shazly M. H., Al-Kabbany A. M., Ali W. Y., Ali A. S. and Massoud M. A., "Effect of Magnetic Field on the Voltage Output of Triboelectric Nanogenerator", Journal of the Egyptian Society of Tribology, Vol. 20, No. 3, July 2023, pp. 85 – 94, (2023).

10. Ali A. S., Youssef M. M., Ali W. Y. and Rashed A., "Triboelectric Nanogenerator Based on Triboelectrification and Magnetic Field", Journal of the Egyptian Society of Tribology, Vol. 20, No. 2, April 2023, pp. 1 – 12, (2023).

11. Gabor D., Radu S. M., Ghicioi E., Paraian M., Jurca A. M., Vatavu N., Paun F., and Popa C. M., "Study of methods for assessment of the ignition risk of dust/air explosive atmospheres by electrostatic discharge", Calitatea, Vol. 20, No. S1, p. 93, (2019).

12. Glor M., and Thurnherr P., "Ignition Hazards Caused by Electrostatic Charges in Industrial Processes", Thuba Ltd, (2015).

13. Von Pidoll U., "An overview of standards concerning unwanted electrostatic discharges", Journal of Electrostatics, Vol. 67, No. 2-3, pp. 445 - 452, (2009).

14. Tian H., and Lee J. J., "Electrostatic discharge damage of MR heads", IEEE transactions on magnetics, Vol. 31, No. 6, pp. 2624 - 2626, (1995).

15. Al-Kabbany A. M., and Ali W. Y., "Reducing the Electrostatic Charge of Polyester by Blending by Polyamide Strings", Journal of the Egyptian Society of Tribology, Vol. 16, No. 4, pp. 36 - 44, (2019).
16. Ali A. S., Al-Kabbany A. M., Ali W. Y., and Samy A. M., "Reducing the Electrostatic Charge Generated from Sliding of Rubber on Polyethylene Artificial Turf", Journal of the Egyptian Society of Tribology, Vol. 17, No. 2, pp. 40 - 49, (2020).
17. Ali A. S., El-Sherbiny Y. M., Ali W. Y., and Ibrahem R. A., "Selection of Floor Materials in Hospitals to Resist Covid-19", Journal of the Egyptian Society of Tribology, Vol. 18, No. 1, pp. 40 - 51, (2021).
18. Ali A. S., Al-Kabbany A. M., Ali W. Y., and Badran A. H., "Triboelectrified Materials of Facemask to Resist Covid-19", Journal of the Egyptian Society of Tribology, Vol. 18, No. 1, pp. 52 - 62, (2021).
19. Ali A. S., Al-Kabbany A. M., Ali W. Y., and Ibrahem R. A., "Proper Material Selection of Medical Safety Goggles", Journal of the Egyptian Society of Tribology, Vol. 18, No. 2, pp. 1 - 14, (2021).
20. Al-Kabbany A. M., Ali W. Y., and Ali A. S., "Proposed Materials for Face Masks", Journal of the Egyptian Society of Tribology, Vol. 18, No. 3, pp. 35 - 41, (2021).
21. Al-Kabbany A. M., Ali W. Y., and Ali A. S., "Proper Selection Materials of Face Shields, Eyeglasses and Goggles", Journal of the Egyptian Society of Tribology, Vol. 18, No. 3, pp. 42 - 51, (2021).
22. Furfari F. A., "A history of the Van de Graaff generator", IEEE Industry Applications Magazine, Vol. 11, No. 1, pp. 10–14, (2005).
23. Fan F.-R., Tian Z.-Q., and Wang Z. L., "Flexible triboelectric generator", Nano Energy, Vol. 1, No. 2, pp. 328 - 334, (2012).
24. Goh Q. L., Chee P., Lim E. H., and Liew G. G., "Self-powered pressure sensor based on microfluidic triboelectric principle for human–machine interface applications", Smart Materials and Structures, Vol. 30, No. 7, p. 075012, (2021).
25. Zhang R., Hummelgard M., Ortegren J., Olsen M., Andersson H., Yang ¨ Y., Olin H., and Wang Z. L., "Utilising the triboelectricity of the human body for human-computer interactions", Nano Energy, Vol. 100, , p. 107503, (2022).
26. Yang Y., Zhu G., Zhang H., Chen J., Zhong X., Lin Z.-H., Su Y., Bai P., Wen X., and Wang Z. L., "Triboelectric nanogenerator for harvesting wind energy and as self-powered wind vector sensor system", ACS nano, Vol. 7, No. 10, pp. 9461 - 9468, (2013).
27. Han J., Feng Y., Chen P., Liang X., Pang H., Jiang T., and Wang Z. L., "Wind-driven soft-contact rotary triboelectric nanogenerator based on rabbit fur with high performance and durability for smart farming", Advanced Functional Materials, Vol. 32, No. 2, p. 2108580, (2022).
28. Zhang H., Yang Y., Su Y., Chen J., Adams K., Lee S., Hu C., and Wang Z. L., "Triboelectric nanogenerator for harvesting vibration energy in full space and as self-powered acceleration sensor", Advanced Functional Materials, Vol. 24, No. 10, pp. 1401 - 1407, (2014).
29. Cheng P., Guo H., Wen Z., Zhang C., Yin X., Li X., Liu D., Song W., Sun X., Wang J., et al., "Largely enhanced triboelectric nanogenerator for efficient harvesting of water wave energy by soft contacted structure", Nano Energy, Vol. 57, pp. 432 - 439, (2019).

30. Meng B., Tang W., Too Z.-h., Zhang X., Han M., Liu W., and Zhang H., "A transparent single-friction-surface triboelectric generator and selfpowered touch sensor", Energy & Environmental Science, Vol. 6, No. 11, pp. 3235 - 3240, (2013).
31. Lei H., Xiao J., Chen Y., Jiang J., Xu R., Wen Z., Dong B., and Sun X., "Bamboo-inspired self-powered triboelectric sensor for touch sensing and sitting posture monitoring", Nano Energy, Vol. 91, p. 106670, (2022).
32. Pu X., Tang Q., Chen W., Huang Z., Liu G., Zeng Q., Chen J., Guo H., Xin L., and Hu C., "Flexible triboelectric 3D touch pad with unit subdivision structure for effective XY positioning and pressure sensing", Nano Energy, Vol. 76, p. 105047, (2020).
33. Haque R. I., Chandran O., Lani S., and Briand D., "Self-powered triboelectric touch sensor made of 3D printed materials", Nano Energy, Vol. 52, pp. 54 - 62, (2018).
34. Chen Y., Cheng Y., Jie Y., Cao X., Wang N., and Wang Z. L., "Energy harvesting and wireless power transmission by a hybridized electromagnetic–triboelectric nanogenerator", Energy & Environmental Science, Vol. 12, No. 9, pp. 2678 - 2684, (2019).
35. Quan T., Wang Z. L., and Yang Y., "A shared-electrode-based hybridized electromagnetic-triboelectric nanogenerator", ACS Applied Materials & Interfaces, Vol. 8, No. 30, pp. 19 573 - 19 578, (2016).
36. Qin K., Chen C., Pu X., Tang Q., He W., Liu Y., Zeng Q., Liu G., Guo H., and Hu C., "Magnetic array assisted triboelectric nanogenerator sensor for real-time gesture interaction", Nano-micro letters, Vol. 13, pp. 1 - 9, (2021).
37. Ali A. S., Al-Kabbany A. M., and Ali W. Y., "Voltage Generated From Triboelectrification of Rabbit Fur and Polymeric Materials", Journal of the Egyptian Society of Tribology, Vol. 19, No. 3, pp. 10 - 18, (2022).
38. Zhang R., and Olin H., "Material choices for triboelectric nanogenerators: a critical review", EcoMat, Vol. 2, No. 4, p. e12062, (2020).
39. Sow, M., Lacks, D. J., Sankaran, R. M., "Effects of material strain on triboelectric charging: Influence of material properties", Journal of Electrostatics 71 pp. 396 – 399, (2013).
40. Park C. H., Park J. K., Jeon H. S., Chu B. C., "Triboelectric series and charging properties of plastics using the designed vertical-reciprocation charger", J. Electrostat, 66, pp. 578 – 583, (2008).